Phase transitions in highly asymmetric binary hard-sphere fluids: Fluid-fluid binodal from a two-component mixture theory

A. Ayadim and S. Amokrane
Physique des Liquides et Milieux Complexes, Faculté des Sciences et de Technologie, Université Paris XII, 61 Av. du Général de Gaulle, 94010 Créteil Cedex, France
(Received 16 May 2006; published 7 August 2006)

Fluid-fluid binodals of binary hard-sphere mixtures are computed from the recently proposed fundamental measure functional–mean spherical approximation closure of the two-component Ornstein-Zernike equation. The results, especially in the dense fluid region that was not accessible by previous theoretical methods, are compared with the corresponding ones for the one-component fluid of big spheres with effective potential obtained from the same closure. The general trends are those expected for hard-sphere potentials but small difference are detectable. The overall agreement found validates the equivalence of the two descriptions for size ratios $R=8.5$ or greater.

DOI: 10.1103/PhysRevE.74.021106 PACS number(s): 64.60.−i, 61.20.Gy, 64.70.Fx

I. INTRODUCTION

The binary mixture of hard spheres (HSs) with large difference in size is the simplest model from which one can address several fundamental questions in the physics of complex fluids, including the purely "entropic" phase transitions, the validity of the effective fluid approach, etc. This model which retains only the geometrical asymmetry through the diameter ratio $R=D_2/D_1>1$ is also the first step before a more realistic modeling of actual mixtures. The case $R\gg 1$ is specially important for the theory since it provides, in the simplest situation, a stringent test for simulations, integral equations, or density functional theories. Besides, it may also be directly relevant to the interpretation of the behavior of pseudobinary mixtures of hard-sphere-like colloids, such as sterically stabilized ones or charged ones at high ionic concentration. But despite several studies that brought valuable information since the early work of Asakura-Oosawa [1] and Vrij [2] on the "depletion" forces in colloid-polymer mixtures, the phase diagram of this basic model is not yet definitely established. There are of course several consistent indications that the phase diagram of mixtures with $R\gtrsim 10$ should mainly consist in a broad fluid-solid coexistence domain, and that it should not show a stable fluid-fluid coexistence. Actually, this picture has been established—*in the effective one component approach*—directly by simulations [3,4], and by using [5] the reference hypernetted chain (RHNC) integral equation [6]. The same qualitative features were also obtained in Ref. [7] from first order perturbation theory, although the special features of the effective potential make the latter approach less accurate in the dense fluid region [8]. *In the true mixture approach*, however, the situation is more contrasted. On the one hand, the domain of low packing fractions of the small spheres η_1 is indeed accessible by simulation ($\eta_i=\frac{\pi}{6}\frac{N_i}{V}D_i^3$ is the packing fraction of component i, N_i is the corresponding number of particles, D_i is their diameter, and V is the volume). In this case, the two routes can be compared directly and they have been shown to be equivalent [3]. The lower part of the fluid-solid coexistence curve is thus firmly established. The same is, however, impossible in the domain of packing fractions $(\eta_1,\eta_2)_{F\text{-}F}$ corresponding to the metastable fluid-fluid phase separation predicted for the effective one component fluid, first because it is not possible to sample in this domain the configuration space of the big spheres (see, for example, Ref. [9]) for $R\gg 1$, despite some specialized simulation algorithms that have been proposed [10–13]. Second, analytical calculations based on standard closures of the multi-component Ornstein-Zernike (OZ) integral equations are either strongly dependent on the quality of the closure or they simply do not converge [14,15]. In addition, the density functional theories that are successful for describing the structure of inhomogeneous fluids [16] do not predict phase separation of bulk fluids. If one imposes for this purpose the test particle consistency, one goes back to the nonconvergence problem of integral equations [17]. Finally, the phenomenological theories that can explore the domain $(\eta_1,\eta_2)_{F\text{-}F}$ such as free volume ones [18] or those using empirical equations of state (see Ref. [19]) or virial expansions (see Ref. [20] and references therein) are either mostly qualitative or sensitive to the approximations (see also Refs. [17,21] for the former). However, the consensus is that for sufficiently asymmetric HS mixtures, the trend at low values of η_1 should persist in the domain of higher values relevant to the fluid-fluid metastable transition, as suggested by some analytical or phenomenological approaches. More fundamentally, it is based on the expectation that the worrisome many-body effects would not be strong enough to make the binary mixture behave in a significantly different way from its effective one-component representation with pair interactions. Besides the qualitative argument of the impossible overlap of more than two exclusion spheres in the Asakura-Oosawa model at sufficiently high R, partial tests [3,9,22,23] indeed show that these should be negligible. It is, however, clear that all the previous data for true mixtures with $R\gg 1$, including simulations and analytical ones were indeed obtained for low packing fractions η_1 of the small spheres, or equivalently η_1^b in the reservoir (for $R\gg 1$, η_1^b is roughly speaking the packing fraction in the free volume). In this domain, say $\eta_1^b\lesssim 0.15$ for $R=10$, the effective fluid approach should indeed suffice because the many-body effects are then expected to be unimportant. This is the case for the simulation data for the

fluid-solid binodals [3] and for the solutes radial distribution functions $g_{22}(r)$ [22] which both showed a good agreement with the one-component description. The simulation data were also obtained in Ref. [12] at low η_1. We also recall that until the beginning of the nineties, the consensus was that hard spheres were miscible at all concentrations and diameter ratios, even if the depletion effect was known for quite a long time [1,2]. This conclusion was drawn from the analytical solution of the Percus-Yevick (PY) closure obtained by Lebowitz and Rowlinson [24]. This question was revisited in 1991 after Biben and Hansen [14] suggested from structural data computed with the Ballone, Pastore, Galli, and Gazzilo [25] (BPGG) and the Rogers and Young [26] (RY) closures a phase instability for $R \gtrsim 5$. Short after that, Rosenfeld [17] computed from the compressibility route a "spinodal" by using his "fundamental measure functional" [16] (FMF) in the density functional theory (DFT) to generate the bridge functions (hereafter this will be referred to as the RHNC-FMF closure and the corresponding version of DFT will be designated as the FMT). Later, free energy calculations [15] with the RY closure were also interpreted as corroborating an instability of the fluid phase. These studies were, however, not conclusive either because of a strong dependence on the specific closure used (spinodal [14,17]) and or because the no-solution domain covers most of the relevant $(\eta_1, \eta_2)_{F\text{-}F}$ range (binodal [15]). We finally mention other studies from the RY closure relative to colloid-star polymers [27] and star polymers mixtures [28] in the two- and one-component descriptions. However, the situations investigated involved either moderate asymmetry or low values of η_1^b and are thus different from those considered here (see also Ref. [29] for another discussion of the RY closure for mixtures). The many-body effects should of course require relatively long range interactions, as in charged colloids, for example. However, the proof of the adequacy of the effective fluid approach will remain, strictly speaking, incomplete until the relevant domain becomes explorable by simulation [30]. In the absence of this proof, we show in this paper the existence of a fluid-fluid phase separation of binary HS mixtures, in the same region $(\eta_1, \eta_2)_{F\text{-}F}$ as for the effective fluid. This will be done by using the special closure of the two-component mixture OZ integral equation that we have recently proposed [31]. As a corollary, this will extend to the nontrivial dense domain, typically $0.35 \lesssim \eta_1 + \eta_2 \lesssim 0.7$ for $R=10$, the validation of the effective one-component fluid with pair interactions approach, and confirm that the fluid-fluid transition is indeed metastable. This paper is hence organized as follows: In Sec. II, we present the theoretical method used to study the phase diagram. The results for the binodals are presented in Sec. III and a brief conclusion is given in Sec. IV.

II. THEORY

In this section, we present the method used to obtain the phase diagram of the mixture, starting with the computation of structural quantities. We first briefly recall the closure we proposed [31] to this end. This was achieved by means of a compromise between accuracy and reduction of the no-solution domain, that made the range $(\eta_1, \eta_2)_{F\text{-}F}$ accessible to the integral equation, and this with some confidence. We thus need to supply the multicomponent OZ equations relating the total correlation functions $h_{ij}=g_{ij}-1$ to the direct correlation functions (dcf) c_{ij},

$$h_{ij} = c_{ij} + \sum_k \rho_k c_{ik} \otimes h_{kj}, \tag{1}$$

where $\otimes$ designates a convolution product: $[f \otimes g](\mathbf{r}) = \int d\mathbf{r}' f(\mathbf{r}') * g(\mathbf{r}' - \mathbf{r})$ with a closure,

$$g_{ij} = \exp\{-\beta u_{ij} + h_{ij} - c_{ij} - b_{ij}\}, \tag{2}$$

involving some approximation for the bridge function b_{ij} (with u_{ij} the interaction potentials, $\beta = 1/k_B T$ where T is the temperature). In the original RHNC-FMF closure, all the bridges functions in Eq. (2) are taken from the FMT [16]. However, with this very accurate closure, the no-solution domain covers [17] all the relevant $(\eta_1, \eta_2)_{F\text{-}F}$ range. In order to reduce it, the full RHNC-FMF closure must be abandoned. By extending Rosenfeld's analysis [16] of the convergence of the RHNC-FMF equation, we thus proposed the following modification [31]:

$$c_{11}(r > D_1) = c_{11}^{(0)}(r) + (g_{11}^{(1)} - g_{11}^{(0)}); \quad g_{11}(r \leqslant D_1) = 0, \tag{3}$$

$$c_{12}(r > D_{12}) = c_{12}^{(0)}(r) + (g_{12}^{(1)} - g_{12}^{(0)}); \quad g_{12}(r \leqslant D_{12}) = 0, \tag{4}$$

$$g_{22} = \exp\{-\beta u_{22} + h_{22} - c_{22} - b_{22}\}. \tag{5}$$

$c_{11}^{(0)}(r)$ and $c_{12}^{(0)}(r)$ are the direct correlation functions obtained from the free energy functional consistent [32,33] with the equation of state of Boublik, Mansoori, Carnahan, Starling, and Leland (BMCSL) [34]. The associated radial distribution functions $g_{11}^{(0)}$ and $g_{12}^{(0)}$ are computed by Fourier transforms, using the Ornstein-Zernike Eq. (1). With $g_{11}^{(0)}$ and $g_{12}^{(0)}$ as input in the density profile (DP) equation,

$$g_{ti}^{DP}(r) = \exp\{-\beta[u_{ti}(r) + \mu_{i,ex}[\{\rho_i(r)\}; r] - \mu_{i,ex}(\{\rho_i\})]\}, \tag{6}$$

one computes $g_{11}^{(1)}(r) = g_{11}(\Delta\mu_{11}^{HS}[\{g_{i1}^{(0)}(r); r\}])$ and $g_{12}^{(1)}(r) = g_{12}(\overline{\Delta\mu}_{12}^{HS}[\{g_{i2}^{(0)}(r); r\}])$ (as indicated by the superscript (1), this corresponds to the first step in a pure DFT calculation). Here, $\Delta\mu_{it}^{HS} = \mu_{i,ex}^{HS}[\{\rho_i g_{it}(\mathbf{r}); \mathbf{r}\}] - \mu_{i,ex}^{HS}(\{\rho_i\})$, where $\mu_{i,ex}^{HS}$ is the excess chemical functional and t is the test particle. For unlike spheres, it is symmetrized [31] as

$$\overline{\Delta\mu}_{12} = (\eta_2 \Delta\mu_{12}^{HS} + \eta_1 \Delta\mu_{21}^{HS})/(\eta_1 + \eta_2). \tag{7}$$

The closure was designated as the "FMF-MSA" closure since it combines Rosenfeld's "fundamental measure functional" with a mean spherical approximation (MSA) like closure for c_{11} and c_{12}. It is, however, clearly distinct from the latter. Note that the symmetrization (7) uses as weighting factors the packing fractions instead of the concentrations $x_i = N_i/\Sigma N_i$. At least in the context of the modified closure, this was found [31] to work better than other symmetrizations such as Rosenfeld's ansatz:

$$\bar{b}_{12} = (x_1 b_{21} + x_2 b_{12})/(x_1 + x_2), \tag{8}$$

or the alternative one,

$$\bar{b}_{12} = (x_1 b_{12} + x_2 b_{21})/(x_1 + x_2), \tag{9}$$

that were both considered in our previous work [23]. We recall here that in the test particle limit of the density profile equation, the bridge function b_{it} is obtained as

$$b_{it}(r) = B_i[\{\rho_m g_{mt}(r); r\}], \tag{10}$$

where the bridge functional B_i—relative to component i—is a functional of all the pair distribution functions (PDFs) g_{mt} in the field of the test particle t. Comparison with simulation and RHNC and DFT data has shown that this closures gives a very accurate description of the structure [31]. With the exception of the full RHNC-FMF closure from which it derives, it is clearly superior to all the closure used so far to study highly asymmetric mixtures (it is even more accurate than the pure DFT [31]). Its major advantage is its much smaller no-solution domain compared with the RY, BPGG, or RHNC ones. This allowed us to explore the $(\eta_1, \eta_2)_{F\text{-}F}$ domain and thus compute the fluid-fluid binodal. We recall here that this significant reduction of the no-solution domain was obtained by relaxing the "constraints" on the integral equation through Eqs. (3) and (4), while essentially preserving the numerical result obtained with the full ("constrained") RHNC closure. Following standard methods [35], we performed the common tangent construction on the isobaric $g(T,p,x_2)$ curves with $G(T,p,x_2,N=N_1+N_2) = Ng(T,p,x_2)$ the Gibbs free energy, p the pressure, and x_2 the big spheres concentration. $g(T,p,x_2)$ was computed from the virial route as $g=f+p/\rho$ with f the Helmholtz free energy per particle:

$$\beta g(T,p,x_2) = \int_0^{\rho(P)} \frac{Z(\rho')-1}{\rho'} d\rho' + Z(\rho) + \beta f_{id}(\rho). \tag{11}$$

$f_{id}(\rho) = \Sigma_i x_i \ln(x_i) + \ln(\rho) - 1$ is the free energy per particle of the ideal mixture and $Z = p/(\rho k_B T)$ is the compressibility factor. For hard spheres, it is obtained from the contact values of the PDFs, $g_{ij}(D_{ij})$ as $Z = 1 + \frac{2}{3}\pi\rho\Sigma_{ij} x_i x_j D_{ij}^3 g_{ij}(D_{ij})$. Equations (1) and (3)–(5) must be solved for each state point of the integration path in Eq. (11). The method is thus time consuming but it involves no special difficulty as long as these equations converge (see Ref. [15] for a similar procedure).

The spinodal corresponds to the vanishing of $\left(\frac{\partial^2 G}{\partial x_2^2}\right)_{N,P,T}$. Its determination in the virial route [using Eq. (11)] is a nontrivial numerical task and we do not undertake it here. In contrast, it is readily obtained in the compressibility route from the Fourier transforms $\tilde{c}_{ij}(k)$ of $c_{ij}(r)$ using the (formally) exact relation

$$S_{cc}(k=0) = \frac{N k_B T}{\left(\frac{\partial^2 G}{\partial x_1^2}\right)_{N,P,T}} \tag{12}$$

with $S_{cc}(k) = x_1 x_2 [x_2 S_{11}(k) + x_1 S_{22}(k) - 2\sqrt{x_1 x_2} S_{12}(k)]$ where $S_{ij}(k)$ are the partial structure factors. The spinodal corresponds to the divergence of $S_{cc}(k)$ or equivalently via the OZ equations to the equation

$$D(k=0) \equiv [1 - \rho_1 \tilde{c}_{11}(k=0)][1 - \rho_2 \tilde{c}_{22}(k=0)] - \rho_1 \rho_2 \tilde{c}_{12}^2(k=0) = 0. \tag{13}$$

Since the vanishing of $D(k=0)$ may actually occur beyond the limit of the convergence domain, a practical criterion used to diagnose a possible spinodal is the behavior of the quantity $\Lambda = x_1 x_2 / S_{cc}(k=0)$. At fixed η_1^b it shows an abrupt variation with η_2 near the spinodal, allowing thus its accurate location by extrapolation [14,17]. This much faster method is, however, subject to a possible thermodynamic inconsistency of the specific closure used. Since our purpose here is not a thorough discussion of the spinodal, we will discuss below only the compressibility route.

Finally, the thermodynamics of the effective fluid is determined by computing the effective-pair potential for big spheres at infinite dilution from the the same closure. Taking the limit $\rho_2 \to 0$ in Eq. (1) one gets

$$\gamma_{11} = c_{11} + \rho_1 c_{11} \otimes h_{11}. \tag{14}$$

h_{11} is used the equation

$$\gamma_{21} = c_{21} + \rho_1 c_{21} \otimes h_{11} \tag{15}$$

to obtain h_{21} and c_{21} from which one computes

$$\gamma_{22} = c_{22} + \rho_1 c_{21} \otimes h_{21}. \tag{16}$$

The effective potential is then

$$\beta\phi^{eff}(r;\mu_1) = \beta\phi_{22}^{HS} - \gamma_{22}(r) + b_{22}(r). \tag{17}$$

The RHNC closure for a one component fluid is then used to compute the binodal corresponding to ϕ^{eff} (see Ref. [5] for details). The correspondence with the binary mixture is then made by directly solving the osmotic equilibrium equation

$$\mu_1(\eta_1^b) = \mu_1(\eta_1, \eta_2). \tag{18}$$

The chemical potential μ_1 for the one-component fluid was taken from the Carnahan-Starling expression [34] and $\mu_1(\eta_1, \eta_2)$ was obtained by numerical differentiation around the known coexistence values of x_2 as $\mu_1 = g(T,p,x_2) - x_2(\partial g/\partial x_2)_{T,P}$. From this procedure, we readily perform the mapping $(\eta_1, \eta_2) \to (\eta_1^b, \eta_2)$. The converse $(\eta_1^b, \eta_2) \to (\eta_1, \eta_2)$ is more difficult numerically, but it can be estimated by using expressions such as that proposed in Ref. [36]. This is, however, not strictly consistent with the actual theory used to obtain $\mu_1(\eta_1, \eta_2)$ for the binary mixture. We will thus perform here only the first mapping.

III. RESULTS AND DISCUSSION

A. Spinodal

Before presenting the results for the binodal we briefly discuss here the compressibility spinodal estimated from the full RHNC-FMF closure. Figure 1(a) shows the evolution with η_2 of the parameter Λ used to diagnose the spinodal. Its behavior is obviously dependent on the details of the calcu-

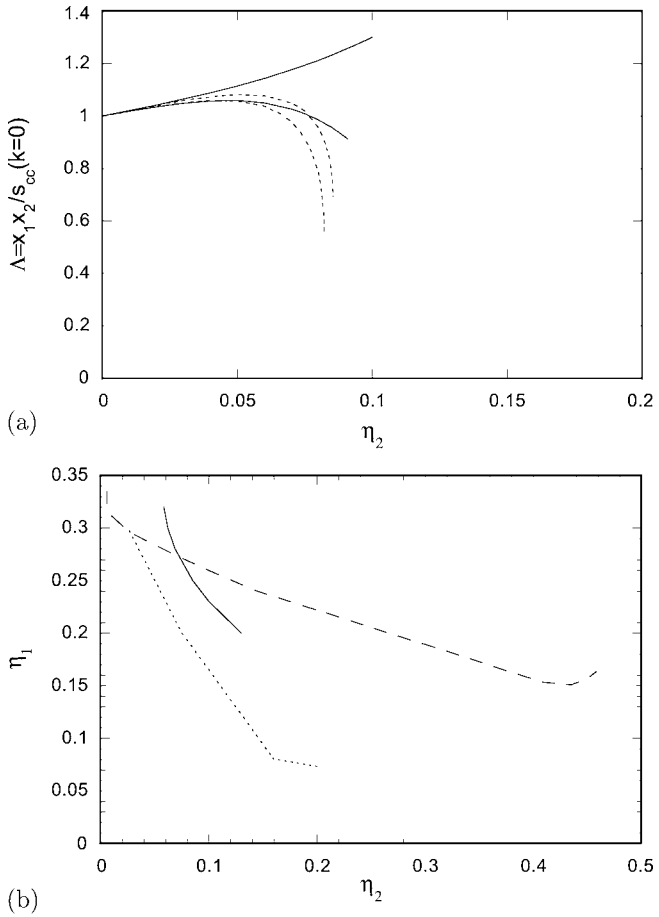

FIG. 1. (a) Ratio $\Lambda=x_1x_2/S_{cc}(0)$ for $R=10$ and $\eta_1^b=0.16$ from the RHNC-FMF closure with different bridges cycles and symmetrizations. Dotted lines: first bridge cycle. Full lines: fully converged RHNC-FMF calculation. In each set the lower curves are obtained with the symmetrization (8) [see also Fig. 1 in Ref. [17] (b) and the upper curves with the symmetrization (9)]. (b) Estimated compressibility spinodals for $R=10$ from the RHNC-FMF closure. Dotted line: original free energy functional [17] and Eq. (8). Full line: modified functional [32,33] and Eq. (9). The dashed line shows the *binodal* of the effective fluid from Ref. [3].

lation. Besides the nonconvergence problem which complicates the discussion, the compressibility route is found to be very sensitive to minute changes in the different terms of Eq. (13). This includes the type of symmetrization, the precise free energy functional, or the number of iterations as illustrated in Tables I and II. Near the no solution boundary, the values of the structural quantities and hence of Λ are subject

TABLE I. Components of the determinant $D(k=0)$ for $R=10$ used to estimate the spinodal as in Ref. [17] from Eqs. (3), (4) and a similar equation for c_{22}.

η_1	η_2	$1-\rho_1 c_{11}$	$1-\rho_2 c_{22}$	$\rho_1\rho_2 c_{12}^2$	$D(k=0))$
	0.389	51.636	$19.018\ 10^3$	$98.27\ 10^4$	$-6.99\ 10^2$
0.25	0.390	52.059	$19.276\ 10^3$	100.3810^4	$-3.07\ 10^2$
	0.391	52.486	$19.538\ 10^3$	$102.54\ 10^4$	$1.02\ 10^2$

TABLE II. Components of the determinant $D(k=0)$ for $R=10$ from the RHNC-FMF closure with different bridges cycles and symmetrizations. Lines 1–3: first bridge cycle and Eq. (8); lines 4–6: fully converged RHNC-FMF calculation with same symmetrization; lines 7–9: fully converged RHNC-FMF calculation with symmetrization (9).

$\eta_1/(1-\eta_2)$	η_2	$1-\rho_1 c_{11}$	$1-\rho_2 c_{22}$	$\rho_1\rho_2 c_{12}^2$	$D(k=0)$
	0.080	3.5008	74.633	257.90	3.372
0.16	0.081	3.4951	75.678	261.36	3.144
	0.082	3.4819	76.714	264.43	2.681
	0.080	3.5346	74.625	259.51	4.262
0.16	0.081	3.5353	75.675	263.28	4.251
	0.082	3.5360	76.729	267.08	4.239
	0.080	3.5373	74.334	262.94	5.251
0.16	0.081	3.5381	75.376	266.69	5.283
	0.082	3.5389	76.422	270.45	5.316

to other numerical uncertainties (see the discussion in Ref. [37] for one-component fluids or less asymmetric mixtures), such as the mesh size, etc. Here for $R=10$ we used $N=16\ 384$ and $dr=0.01D_1$ in order to minimize them. It seems difficult to go beyond these values but they are sufficient for the qualitative aspects discussed in this section. Spinodals estimated from the the full RHNC closure are shown in Fig. 1(b). For comparison with Rosenfeld's calculation [17], we include the result obtained by always keeping in the closure the bridge functions computed with the input correlation functions $c_{ij}^{(0)}(r)$ and $g_{ij}^{(0)}(r)$ (first bridge cycle). We note that the "spinodal " estimated in this way lies well below the *F-F* binodal for the effective fluid and differs significantly from the one estimated with the modified functional and a different symmetrization of the bridge function b_{12}. For all these reasons we think that, as long as we lack a closure that is both accurate and respects the consistency between the various thermodynamic routes, the compressibility route is not a viable one for studying the spinodal in highly asymmetric mixtures. With the modified closure that is less subject to the nonconvergence limitation, it should be possible to compute a virial spinodal. This, however, remains a difficult numerical task [31], that we leave for future work. In the coming section, we will discuss the binodal computed from the virial route only, essentially because of this great sensitivity of the compressibility route.

B. Binodal

We first recall the challenge by showing in Fig. 2 the full phase diagram of the effective fluid obtained by Monte Carlo (MC) simulations [3] and from [5] the reference hypernetted chain (RHNC) integral equation [6], for the potential of Götzelmann, Evans, and Dietrich (GED) [38] for $R=10$). Note that consistently with the version of Lado using the standard RHNC free energy, as the RHNC-FMF used here (in contrast with alternative treatments of the nonlocal term—see Ref. [5] for details), the more recent simulation data [30] suggest that the critical value $\eta_{1,c}^b$ is somewhat overestimated by the

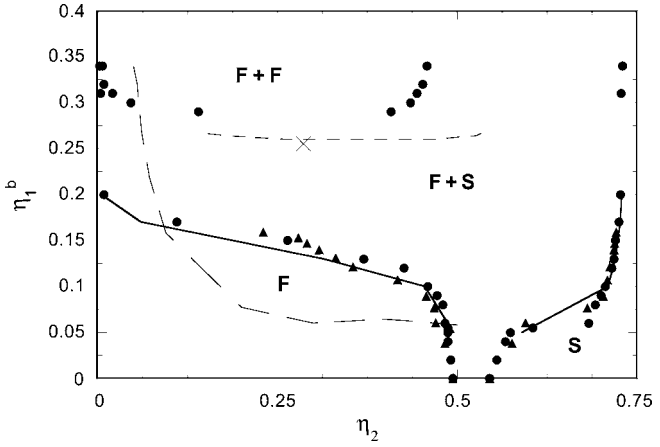

FIG. 2. Phase diagram of a hard-sphere mixture with $R=10$. Symbols: simulation data of Ref. [3]: circles: one-component fluid; triangles: binary mixture. Lines: RHNC integral equation: full line: fluid-solid binodal [5], short dashed line fluid-fluid binodal from the "Lado version" [5] (data from Ref. [5] are for the one-component fluid with the GED potential of Götzelmann *et al.* [38]). The cross shows the critical point obtained by simulation in Ref. [30]. Long dashes: boundary of the no-solution domain (above this line) of the RHNC-FMF closure [true mixture and mapping $(\eta_1, \eta_2) \rightarrow (\eta_1^b, \eta_2)$ from Ref. [36]].

method used in Ref. [3]. The point here is that the fluid-fluid binodal lies completely inside the no-solution domain of the original RHNC-FMF closure. This was the main motivation of our search of a more flexible closure [31].

The binodal for the binary mixture with $R=10$ obtained from the FMF-MSA closure is compared with the corresponding one in the effective fluid in Fig. 3, using the mapping $(\eta_1, \eta_2) \rightarrow (\eta_1^b, \eta_2)$ from Eq. (18). We first notice the non-completely-trivial result that a fluid-fluid binodal is indeed predicted by the treatment of the two-component mixture by the FMF-MSA closure. This binodal is similar to that determined for the effective fluid, with FMF-MSA effective potential treated with the RHNC closure. Its closeness with the simulations [3] for the GED potential is subject to the remark made above. Differences are, however, detectable at high η_2, and are possible for the critical value η_2^c. The latter is, however, difficult to estimate since the binodal is very flat. The binodal is finally far from the compressibility spinodal obtained in Ref. [17]. This is understandable from the reasons discussed in the previous section. The binodals for $R=8.5$ and $R=10$ are compared in Fig. 4. The ordering in Fig. 4(a) is the one expected. Notice that in an exploratory study for $R=7$ we could not find a binodal until high pressure values at which the convergence becomes extremely difficult. This absence remains, however, to be confirmed. For $R=8.5$, the difference between the effective fluid and the true binary mixture is more apparent, which is in line with the expected increase of the many-body effects when the asymmetry decreases, but both remain rather close. In the absence of simulation data for the binodal, we compare in

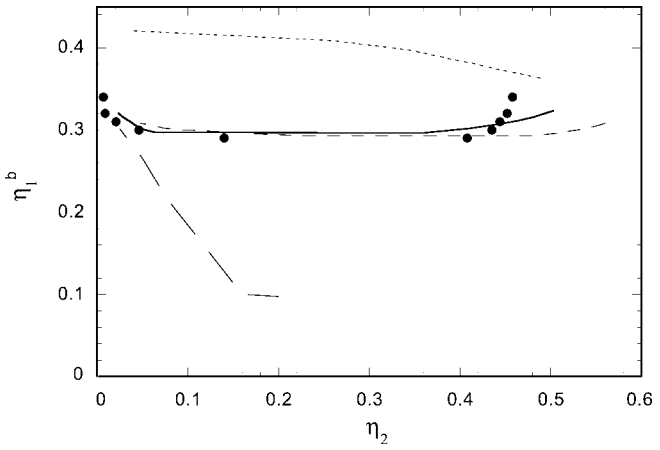

FIG. 3. Fluid-fluid binodal of a hard-sphere mixture with $R=10$ in the one-component representation. Circles: simulation data of Ref. [3] with the GED potential, *effective fluid*. Full line: FMF-MSA fluid-fluid binodal of the true mixture converted with the osmotic equilibrium equation. Short dashes: fluid-fluid binodal of the *effective fluid* with FMF-MSA effective potential. Long dashed line: RHNC-FMF "spinodal" from Ref. [17]. Dotted line: estimated no-solution boundary of the FMF-MSA closure.

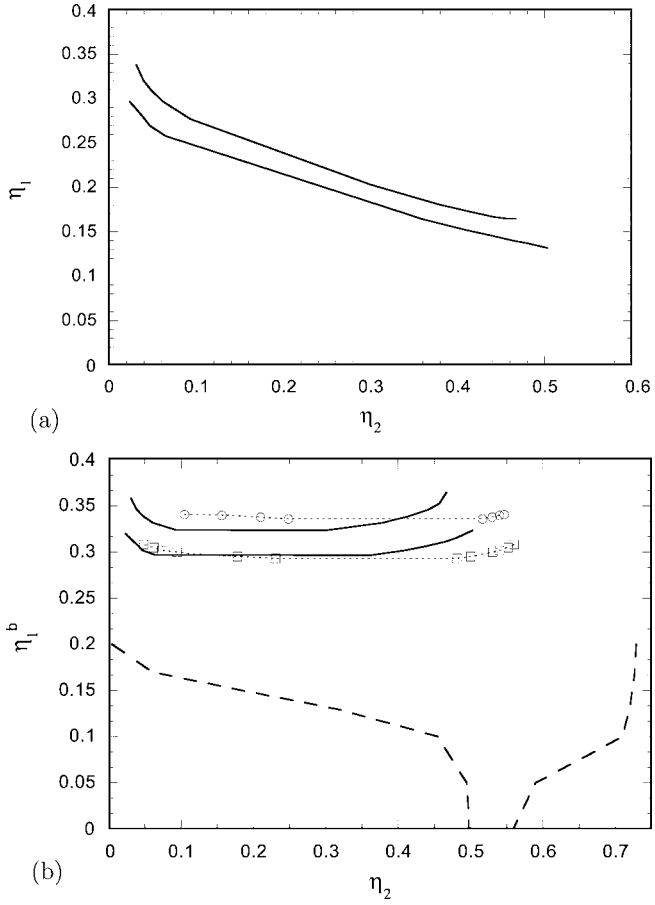

FIG. 4. (a) Fluid-fluid binodal of hard-sphere mixtures with $R=8.5$ and $R=10$ in the (η_1, η_2) plane. The upper curve is for $R=8.5$. (b) Fluid-fluid binodal of hard-sphere mixtures with $R=8.5$ and $R=10$ in the (η_1^b, η_2) plane. Full lines: FMF-MSA fluid-fluid binodal of the true mixture as in Fig. 4(a). Dotted curves with symbols, corresponding one-component fluid with FMF-MSA effective potential. For comparison the fluid-solid boundary for $R=10$ is shown by the dashed line.

TABLE III. Compressibility factor and excess chemical potential from this work and simulation [12].

			FMF−MSA		*DFT*		*MC*	
x_2	$\eta_1+\eta_2$	η_1	Z	μ_1^{ex}	Z	μ_1^{ex}	Z	μ_1^{ex}
0.02	0.35	0.0163	2.0361	0.8134	2.0214	0.8065	2.031	0.812
0.02	0.5	0.0234	3.3322	1.4513	3.3206	1.453	3.331	1.435
0.01	0.35	0.0315	2.109	0.9905	2.106	0.989	2.111	0.99
0.01	0.5	0.045	3.5268	1.8289	3.5081	1.8175	3.532	1.836
0.005	0.35	0.0581	2.3069	1.3277	2.2994	1.3254	2.304	1.346
0.005	0.5	0.083	4.0753	2.5674	4.0376	2.5470	4.067	2.549

Table III some data for the compressibility factor and the chemical potential with those of Ref. [12]. These data confirm the excellent behavior of the FMF-MSA closure. Besides the good accuracy of the structural and thermodynamic quantities computed with the closure in Eqs. (3)–(5), it would be very difficult to imagine that the agreement between the binodal computed for the effective fluid and the binary mixture, in location, shape, and extent could be fortuitous.

IV. CONCLUSION

These results show directly a fluid-fluid binodal in highly asymmetric HS mixture. Together with the direct comparison of the two representations of HS mixtures in the low η_1 regime [3] and the general arguments on the importance of the many-body effects, this validates the effective fluid description of asymmetric HS mixtures, in the nontrivial *dense fluid* region, and at the level of the thermodynamics. The characteristics of the fluid-fluid binodal are thus very important from the point of view of the theory of asymmetric mixtures. Besides, this result confirms the efficiency of the method we have used. Now, since the fluid-fluid transition should be metastable with respect to the fluid-solid one, there is no direct practical exploitation of this result, unless one reaches the metastability domain (for kinetic reasons for example), and this for truly hard-sphere-like colloids. It should then be recalled that some experiments with mixtures of such colloids indicate that the phase coexistence should indeed be between a fluid and a solid [39] (ordered or amorphous). On the other hand, slight deviations from the ideal HS behavior might have a significant effect on the phase behavior [40]—see, for example, the glass transition [41] induced by the addition of polymers in a mixture of HS-like particles. Therefore as illustrated here for hard spheres, the exploration of the dense fluid region remains an important task for a complete description of the phase diagram, even when non-HS contributions to the interactions are deemed to be negligible. For more general interactions, and in the absence of general criteria, the equivalence of both descriptions can be assessed only by explicit calculations. In this respect, the generic nature of the OZ equations/closure route should facilitate this task. Modifications in the spirit of the "relaxed constraint" that motivated the proposed modification of the RHNC closure remain, however, to be devised so as to overcome a possible nonconvergence problem in a specific situation. Work on this aspect is currently in progress.

[1] S. Asakura and F. Oosawa, J. Chem. Phys. **22**, 1255 (1954).
[2] A. Vrij, Pure Appl. Chem. **48**, 471 (1976).
[3] M. Dijkstra, R. Roij and R. Evans, Phys. Rev. Lett. **81**, 2268 (1998); **82**, 117 (1999); Phys. Rev. E **59**, 5744 (1999).
[4] N. G. Almarza and E. Enciso, Phys. Rev. E **59**, 4426 (1999).
[5] J. Clement-Cottuz, S. Amokrane, and C. Regnaut, Phys. Rev. E **61**, 1692 (2000).
[6] F. Lado, S. M. Foiles, and N. W. Ashcroft, Phys. Rev. A **28**, 2374 (1983).
[7] E. Velasco, G. Navascuès, and L. Mederos, Phys. Rev. E **60**, 3158 (1999).
[8] Ph. Germain and S. Amokrane, Phys. Rev. E **65**, 031109 (2002).
[9] T. Biben, P. Bladon, and D. Frenkel, J. Phys.: Condens. Matter **8**, 10799 (1996).
[10] J. I. Siepmann and D. Frenkel, Mol. Phys. **75**, 59 (1992).
[11] W. Krauth, in *Advance in Computer Simulation*, Lecture Notes in Physics, edited by J. Kertesz and I. Kondor (Springer-Verlag, Berlin, 1998); C. Dress and W. Krauth, J. Phys. A **28**, L597 (1995); A. Buhot and W. Krauth, Phys. Rev. Lett. **80**, 3787 (1998).
[12] L. Lue and L. V. Woodcock, Mol. Phys. **96**, 143 (1999).
[13] J. Liu and E. Luijten, Phys. Rev. E **71**, 066701 (2005).
[14] T. Biben and J. P. Hansen, Phys. Rev. Lett. **66**, 2215 (1991).
[15] C. Caccamo and G. Pellicane, Physica A **235**, 149 (1997).
[16] Y. Rosenfeld, J. Chem. Phys. **98**, 8126 (1993).
[17] (a) Y. Rosenfeld, Phys. Rev. Lett. **72**, 3831 (1994); (b) J. Phys. Chem. **99**, 2857 (1995).
[18] H. N. W. Lekkerkerker and A. Stroobants, Physica A **195**, 387 (1993); H. N. W. Lekkerkerker, W. C. K. Poon, P. N. Pusey, A. Stroobants, and P. B. Warren, Europhys. Lett. **20**, 559 (1992); H. N. W. Lekkerkerker and S. Martijn Oversteegen, J. Phys.: Condens. Matter **14**, 9317 (2002).
[19] D. Henderson, D. Boda, K. Y. Chan, and T. Wasan, Mol. Phys. **95**, 131 (1998); C. Regnaut, A. Dyan, and S. Amokrane, *ibid.* **99**, 2055 (2001); S. B. Yuste, A. Santos, and M. López de

Haro, Europhys. Lett. **52**, 158 (2000).
[20] M. López de Haro and C. F. Tejero, J. Chem. Phys. **121**, 6918 (2004).
[21] S. Amokrane and C. Regnaut, Phys. Rev. E **53**, 1990 (1996).
[22] J. G. Malherbe and S. Amokrane, Mol. Phys. **99**, 355 (2001).
[23] S. Amokrane, A. Ayadim, and J. G. Malherbe, J. Phys.: Condens. Matter **15**, S3443 (2003).
[24] J. L. Lebowitz and J. S. Rowlinson, J. Chem. Phys. **41**, 133 (1964).
[25] P. Ballone, S. Pastore, G. Galli, and D. Gazzilio, Mol. Phys. **59**, 275 (1986).
[26] F. J. Rogers and D. A. Young, Phys. Rev. A **30**, 999 (1984).
[27] J. Dzubiella, C. N. Likos, and H. Löwen, J. Chem. Phys. **116**, 9518 (2002).
[28] C. Mayer, C. N. Likos, and H. Löwen, Phys. Rev. E **70**, 041402 (2004).
[29] C. Caccamo, R. Ricciai, G. Pellicane, and G. Faggio, J. Phys.: Condens. Matter **12**, 2613 (2000).
[30] J. Largo and N. B. Wilding, Phys. Rev. E **73**, 036115 (2006).
[31] S. Amokrane, A. Ayadim, and J. G. Malherbe, J. Chem. Phys. **123**, 174508 (2005).
[32] Y. Yu and J. Wu, J. Chem. Phys. **117**, 10156 (2002).
[33] R. Roth, R. Evans, A. Lang, and G. Kahl, J. Phys.: Condens. Matter **14**, 12063 (2002).
[34] T. Boublik, J. Chem. Phys. **53**, 471 (1970); G. A. Mansoori, N. F. Carnahan, K. E. Starling, and T. W. Leland, Jr, *ibid.* **54**, 1523 (1971).
[35] J. S. Rowlinson, *Liquids and Liquid Mixtures* (Butterworths, London, 1969).
[36] R. Roth, R. Evans, and A. A. Louis, Phys. Rev. E **64**, 051202 (2001).
[37] L. Belloni, J. Chem. Phys. **98**, 8080 (1993).
[38] B. Götzelmann, R. Evans, and S. Dietrich, Phys. Rev. E **57**, 6785 (1998).
[39] A. D. Dinsmore, A. G. Yodh, and D. J. Pine, Phys. Rev. E **52**, 4045 (1995); A. Imhof and J. K. G. Dhont, Phys. Rev. Lett. **75**, 1662 (1995); Y. Hennequin, M. Pollard, and J. S. van Duijneveldt, J. Chem. Phys. **120**, 1097 (2004).
[40] Ph. Germain, J. G. Malherbe, and S. Amokrane, Phys. Rev. E **70**, 041409 (2004).
[41] T. Eckert and E. Bartsch, Phys. Rev. Lett. **89**, 125701 (2002).